Old Dominion University Research Foundation

DEPARTMENT OF MECHANICAL ENGINEERING
COLLEGE OF ENGINEERING AND TECHNOLOGY
OLD DOMINION UNIVERSITY
NORFOLK, VA 23529

NONLINEAR TRANSIENT PROBLEMS USING STRUCTURE-COMPATIBLE HEAT TRANSFER CODE

By
Dr. Gene Hou, Principal Investigator
Department of Mechanical Engineering

FINAL REPORT

For the period ending June 30, 1999

Prepared for
NASA Langley Research Center
Attn.: Dr. Kim S. Bey
Technical Officer
Mail Stop 396
Hampton, VA 23681-2199

Under
NASA NAG-1-1985
ODURF File No. 180190

January 2000

Final Report

NASA NAG-1-1985
ODURF No. 180190

Nonlinear Transient Problems Using Structure-Compatible Heat Transfer Code

By
Dr. Gene Hou, Principal Investigator
Department of Mechanical Engineering
Old Dominion University

Submitted by
Old Dominion University
Research Foundation
800 West 46th Street
Norfolk, Virginia 23508

Submitted to
NASA Langley Research Center
Hampton, VA 23681-2199

January 2000

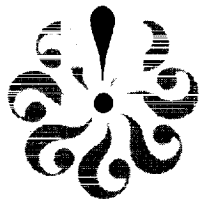

NONLINEAR TRANSIENT PROBLEMS USING STRUCTURE - COMPATIBLE HEAT TRANSFER CODE

Gene Hou, Yang Wang and Rufeng Liu

Department of Mechanical Engineering
Old Dominion University
Norfolk, VA 23454

The report documents the recent effort to enhance a transient linear heat transfer code so as to solve nonlinear problems. The linear heat transfer code was originally developed by Dr. Kim Bey of NASA Largely and called the Structure-Compatible Heat Transfer (SCHT) code. The report includes four parts. The first part outlines the formulation of the heat transfer problem of concern. The second and the third parts give detailed procedures to construct the nonlinear finite element equations and the required Jacobian matrices for the nonlinear iterative method, Newton-Raphson method. The final part summarizes the results of the numerical experiments on the newly enhanced SCHT code.

I. FORMULATION

The system of the governing differential equations of a heat transfer problem in a homogeneous material can be expressed as

$$\rho c \frac{\partial T}{\partial t} - \sum_{i=1}^{3}\sum_{j=1}^{3} \frac{\partial}{\partial x_i}\left(K_{ij} \frac{\partial T}{\partial x_j} \right) = Q(x,t), \quad \text{in} \quad \Omega \times (0,T] \tag{1}$$

$$u = f(x,t), \quad \text{on} \quad \partial\Omega_u \times (0,T] \tag{2}$$

$$\sum_{i=1}^{3}\sum_{j=1}^{3} K_{ij} \frac{\partial T}{\partial x_j} n_i = q_s(x,t), \quad \text{on} \quad \partial\Omega_q \times (0,T] \tag{3}$$

and

$$u = g(x), \quad \text{in} \quad \Omega \quad \text{at} \quad t = 0 \tag{4}$$

where the temperature, $T(x, t)$, is the only unknown. Equation (1) represents an initial-boundary value problem with Eq. (2) and Eq. (3) being the temperature and the heat flux boundary conditions, respectively, and Eq.(4), the initial conditions. It is assumed that the heat source, Q, the prescribed temperature, f, and the flux, q_s, and the initial value, g, are all with proper regularity. In case of material nonlinearity, the coefficients in Eq.(1), the

specific heat, $\rho c(T)$ and the thermal conductivity, K_{ij} (T) are assumed to be functions of temperature.

The weak form of the above equations can be derived based upon the discontinuous Galerkin method [1] for a time interval, $I_n = [\, t_{n-1}, t_n \,)$ as

$$\int_{t_{n-1}}^{t_n}\left(\int_\Omega\left[\rho c\frac{\partial T}{\partial t}v + K_{ij}\frac{\partial T}{\partial x_i}\frac{\partial v}{\partial x_j}\right]dx\right)dt + \int_\Omega (\rho c)_{n-1}^{+} T_{n-1}^{+} v dx$$

$$= \int_{t_{n-1}}^{t_n}\left(\int_\Omega Q v dx dt\right) + \int_\Omega (\rho c)_{n-1}^{-} T_{n-1}^{-} v dx + \int_{t_{n-1}}^{t_n}\int_{\partial\Omega_q} q_s v ds dt \qquad (5)$$

where the testing function, $v = 0$ on $\partial\Omega_u$ and the temperature be a combination of the unknown function, u, and an arbitrary function, w. The testing function should satisfy the boundary condition, $w = f$, on $\partial\Omega_u$. Consequently, $u = 0$ on $\partial\Omega_u$. Note that u is the only unknown in Eq. (5).

The symbols of T_{n-1}^{-} and T_{n-1}^{+} are the limits of temperatures approach to the point, t_{n-1}, from its right and left sides. It should be noted that the continuity of the temperature, T, is not enforced pointwisely throughout the entire time domain, rather it is enforced at the ends of the time interval in a weighted manner. Furthermore, the coefficients, ρc and K_{ij}, also experience discontinuity at the ends of time intervals, as they are functions of the temperatures, which are allowed to be discontinuous at those points.

II. FINITE ELEMENT EQUATIONS

For simplicity, one will start the derivation with an assumption that the problem is homogeneous. That is, $f = 0$ and $T = u$.

The weak equation defined in Eq. (5) can be discretized as a summation of integrals over individual "finite elements". In this study, the computational domain of such a finite element, V_l, is defined as a product of a spatial domain and a time interval, $\Omega_n \times I_n$. As a result, the discretized equations for time interval, I_n, become

$$\sum_\Omega \int_{t_{n-1}}^{t_n}\left(\left[\rho c\frac{\partial T}{\partial t}v + (\boldsymbol{K}\cdot\nabla_x T)\cdot\nabla_x v\right]dx\right)dt + \sum_{\Omega_n}\int_\Omega \rho c T_{n-1}^{+} v dx$$

$$= \sum_{\Omega} \int_{t_{n-1}}^{t_n} \left(\int_{\Omega_n} Qv d\boldsymbol{x} \right) dt + \sum_{\Omega} \int_{\Omega_n} \rho c T_{n-1}^{-} v d\boldsymbol{x} + \sum_{\partial\Omega} \int_{t_{n-1}}^{t_n} \int_{\partial\Omega_{q,n}} q_s v ds dt \qquad (6)$$

where v is the testing function. The tasks in constructing the equivalent matrix equation of Eq. (6) involve selection of the interpolation functions, approximation of nonlinear material properties and integration of elemental matrices.

Interpolation Functions

Following a similar derivation given in [1], a *hp*-version of interpolation function is introduced here to approximate the solution in the kth element space domain and the (n - 1)th time interval as

$$\boldsymbol{T}(\boldsymbol{x},t) = \boldsymbol{X}(\boldsymbol{x},t)\boldsymbol{a}_{n,k}$$

where $\boldsymbol{X}$ ($\boldsymbol{x}$, t) is the interpolation function vector and $\boldsymbol{a}_{n,k}$ is the "nodal value" vector. More specifically, the interpolation function can be spanned as a tensor product of functions with separable variables as

$$\boldsymbol{X}(\boldsymbol{x},t) = L(x,y) \otimes \psi(t) \otimes \varphi(z)$$

or in the index form,

$$X_m = L_i \psi_j \phi_k$$

The subscript, m, in the above equation follows the relation, $m = (i - 1)\, p\, s + (j - 1)\, s + k$ where p and s are the ranges of subscripts, j and k. In the case of a triangular element, the interpolation function, L_i, can be simply specified as an area coordinate,

$$L_i = a_i + b_i x + c_i y, \qquad i = 1,2,3$$

The interpolation function through the thickness, Δ, is a polynomial of a hierarchical basis. In this study, $\phi(z)$ is given as

$$\phi_0 = \frac{1}{2}\left(1 - 2\frac{z}{\Delta}\right)$$

$$\phi_1 = \frac{1}{2}\left(1 + 2\frac{z}{\Delta}\right)$$

$$\phi_j = \frac{1}{\sqrt{2(2j-1)}}\left(P_j\left(2\frac{z}{\Delta}\right) - P_{j-2}\left(2\frac{z}{\Delta}\right)\right), \qquad j = 2,\ldots, p$$

where z ranges from $\Delta/2$ to $\Delta/2$, and P_j is a Legendre polynomial of degree j.

The interpolation function for the time domain, $\psi(t)$, uses a power polynomial in time. That is,

$$\psi_j = t^j, \qquad j = 0,\ldots, s$$

Nonlinear Approximation

It is assumed that in this study, the relations between the material properties, ρc and K_{ij}, and the temperature are defined in a tabulated form, presented as a result of experiments. Therefore, the material properties can not be explicitly specified as functions of position and time as required by integration. An approximation is thus introduced to overcome such a difficulty.

A single *hp*-element is first divided into regular subdomains. The values of the material properties at the vertices of each subdomain are read out from the given material table based upon the values of the temperature found at those points. The values of the material properties at elsewhere in a subdomain are then obtained through linear interpolation. In this way, the material properties are explicitly approximated as functions of position and time throughout the problem domain.

As an example, the spatial and the time domain of an element can be divided into subdomains as shown in Fig. 1. and the material property, say ρc, can be interpolated linearly in a typical subdomain bounded by [z_1 , z_2] x [t_1 , t_2] as

$$\rho c(x,t) = \left(L(x,y) \otimes N_t(t) \otimes N_z(z)\right)^T \boldsymbol{c}$$

where $\boldsymbol{c}$ is the vector of the nodal values of the material properties that are found through the material table and the nodal values of temperature. The area coordinates are in this

case, a nature choice for linear interpolation functions in x-y plane, $\boldsymbol{L}$ (x, y), because of a triangular domain. Typical linear shape functions can be used to interpolate N_t and N_z as

$$N_t = \begin{Bmatrix} N_{t_1} \\ N_{t_2} \end{Bmatrix} = \begin{Bmatrix} (t_2 - t)/(t_2 - t_1) \\ (t - t_1)/(t_2 - t_1) \end{Bmatrix}$$

$$N_z = \begin{Bmatrix} N_{z_1} \\ N_{z_2} \end{Bmatrix} = \begin{Bmatrix} (z_2 - z)/(z_2 - z_1) \\ (z - z_1)/(z_2 - z_1) \end{Bmatrix}$$

As a result, the vector $\boldsymbol{c}$ has 12 components, which gives an approximation of the temperature field in the subdomain of concern as

$$\begin{aligned} \boldsymbol{c}^T &= (c_1, c_2, c_3, c_4, c_5, c_6, c_7, c_8, c_9, c_{10}, c_{11}, c_{12})^T \\ &= (c_{111}, c_{112}, c_{121}, c_{122}, c_{211}, c_{212}, c_{221}, c_{222}, c_{311}, c_{312}, c_{321}, c_{322})^T \end{aligned}$$

where the first subscript of the notation, c_{ijk}, is associated with the area coordinates, the second with the vertices of a time subdomain and the third with the vertices of a z subdomain. Thus, c_{ijk}, is read from the given material table based upon the value of the temperature evaluated at area nodal point i, time vertex j and z vertex k. As an example, the material property, c_{122}, is obtained at the point (x_1, y_1, z_2) x t_2 as

$$c_{122} = \text{function of } T_{ijk}$$

where

$$\begin{aligned} T_{ijk} &= \boldsymbol{X}^T(x_1, y_1, z_2, t_2)\boldsymbol{a}_{n,k} \\ &= (\boldsymbol{L}(x_1, y_1) \otimes \psi(t_2) \otimes \varphi(z_2))^T \boldsymbol{a}_{n,k} \end{aligned}$$

Matrix Evaluation

Once the interpolation functions are selected and the nonlinear material properties are approximated as explicit functions of position and time, one can proceed to integrate the terms in Eq. (6) to construct the equivalent matrices. The resultant finite element matrix equation for the time interval, I_n , can then be expressed as

$$(\boldsymbol{C}_n + \boldsymbol{K}_n + \boldsymbol{M}_n)\{\boldsymbol{a}_n\} = \{\boldsymbol{q}_n\} + \boldsymbol{M}_{n-1}\{\boldsymbol{a}_{n-1}\} + \{\boldsymbol{b}_n\} \tag{7}$$

where the subscript, n, indicates that the associated matrix or vector is evaluated with functions defined in time interval, I_n . Note that each term in Eq. (7) is corresponding to an integral in Eq. (6). As an example, the capacitance matrix is given as

$$C_n = \sum_{\Omega} \int_{t_{n-1}}^{t_n} \left(\int_{\Omega_n} \rho c \frac{\partial T}{\partial t} v dx \right) dt$$

For a specific element k which includes a triangular slab in space and I_n in time, the elemental capacitance matrix with constant ρc can be further spelled out as

$$C_{n,k} = \int_{t_{n-1}}^{t_n} \left(\int_{\Omega_k} \rho c \boldsymbol{X} \frac{\partial \boldsymbol{X}^T}{\partial t} dx \right) dt$$

$$= \int_{t_{n-1}}^{t_n} \left(\int_{\Omega_k} \rho c \left(\boldsymbol{L}(x,y) \otimes \psi(t) \otimes \varphi(z) \right) \left(\boldsymbol{L}(x,y) \otimes \psi(t) \otimes \psi(2) \right)^T dx \right) dt$$

$$= \int_A \boldsymbol{L}\boldsymbol{L}^T dxdy \otimes \int_{t_{n-1}}^{t_n} \psi \frac{d\psi}{dt}^T dt \otimes \int_{-\frac{\Delta}{2}}^{\frac{\Delta}{2}} \rho c \varphi \varphi^T dz$$

where A is the area of the triangular element. In the case of nonlinear ρc, the elemental $\boldsymbol{C}$ matrix is a function of temperature, $\boldsymbol{T}$, and can be written as

$$\boldsymbol{C}_{n,k}(\boldsymbol{a}_{n,k}) = \int_{t_{n-1}}^{t_n} \left(\int_{\Omega_k} \rho c \boldsymbol{X} \frac{\partial \boldsymbol{X}^T}{\partial t} dx \right) dt$$

$$= \int_{t_{n-1}}^{t_n} \left(\int_{\Omega_k} (\boldsymbol{L} \otimes \boldsymbol{N}_t \otimes \boldsymbol{N}_z)^T \boldsymbol{c} \cdot \boldsymbol{X} \frac{\partial \boldsymbol{X}^T}{\partial t} dx \right) dt$$

$$= \sum_{i=1}^{3} \sum_{j=1}^{2} \sum_{k=1}^{2} \int_{t_{n-1}}^{t_n} \left(\int_{\Omega_k} L_i N_{t_j} N_{z_k} c_{ijk} \boldsymbol{X} \frac{\partial \boldsymbol{X}^T}{\partial t} dx \right) dt$$

$$= \sum_{i=1}^{3} \sum_{j=1}^{2} \sum_{k=1}^{2} c_{ijk}(\boldsymbol{a}_{n,k}) \int_A L_i \boldsymbol{L}\boldsymbol{L}^T dxdy \otimes \int_{t_{j-1}}^{t_i} N_{t_j} \psi \frac{d\psi}{dt}^T dt \otimes \int_{z_{k-1}}^{z_k} N_{z_k} \varphi \varphi^T dz \quad (8)$$

Thus, the elemental capacitance matrix is a summation of the subdomain capacitance matrices. The more subdomains divided in each element, the more computational efforts are required.

III. SOLUTION PROCEDURES

The matrix equation derived above is based upon the discontinuous Galerkin's method and will be solved in a time-marching fashion. In other words, the matrix equation of Eq. (7) will be solved for a time interval at a time, with a_n as unknown and a_{n-1} as known quantities. The value, a_0 , is given as the initial condition. The nonlinear version of Eq.(7) is rewritten below for future reference

$$[C_n(a_n)+K_n(a_n)+M_n(a_n)]\{a_n\}=\{q_n\}+[M_{n-1}(a_{n-1})]\{a_{n-1}\}+\{b_n\}$$

The above equation can be solved by either the fixed point iteration or the Newton-Raphson's method.

The recursive formula for the fixed point iteration is simply given as

$$[C_n(a_n^{i-1})+K_n(a_n^{i-1})+M_n(a_n^{i-1})]\{a_n^{i}\}=\{q_n\}+[M_{n-1}(a_{n-1})]\{a_{n-1}\}+\{b_n\}$$

where the superscript, i , denotes the iteration number. The recursive formula for the Newton-Raphson's method, however, is more complicated and involves Jacobian matrices, J_c , J_k and J_m as

$$\begin{aligned}&[C_n(a_n^{i-1})+K_n(a_n^{i-1})+M_n(a_n^{i-1})+J_c^{i-1}a_n^{i-1}+J_k^{i-1}a_n^{i-1}+J_m^{i-1}a_n^{i-1}]\{\Delta a_n^{i}\}\\&=\{R_n^{i-1}\}\end{aligned} \tag{9}$$

and the solution is updated by

$$a_n^{i}=a_n^{i-1}+\Delta a_n^{i} \tag{10}$$

In the above equation, Δa_n^{i} is the improvement of the solution and R_n^{i-1} is the residual of the nonlinear equation at the i-1 iteration which is defined as

$$\{R_n^{i-1}\}=[C_n(a_n^{i-1})+K_n(a_n^{i-I})+M_n(a_n^{i-1})]\{a_n^{i-1}\}-\{q_n\}[M_{n-1}(a_{n-1})]\{a_{n-1}\}-\{b_n\}$$

Moreover, the Jacobian matrices, J_c , J_k and J_m are obtained by differentiating the coefficient matrices C_n , K_n and M_n with respect to the unknown vector a_n , respectively. This is usually accomplished at the element level. As an example, the Jacobian matrix of the element capacitance matrix is obtained for a typical element (n, k) as

$$J_c a_{n,k}=\left[\frac{\partial C_{n,k}}{\partial T_1}a_{n,k},\frac{\partial C_{n,k}}{\partial T_2}a_{n,k},\ldots\right]$$

where $\partial C_{n,k}/\partial T_l$ is obtained by using Eq. (8) as

$$\frac{\partial C_{n,k}}{\partial T_l} = \frac{\partial}{\partial u_l}\left(\sum_i \sum_j \sum_k \int_A L_i \boldsymbol{L}\boldsymbol{L}^T dA \otimes \int_{t_{n-1}}^{t_n} N_{tj} \boldsymbol{\psi} \frac{\partial \boldsymbol{\psi}^T}{\partial t} dt \otimes \int_{z_{m-1}}^{z_m} N_{zk} c_{ijk} \boldsymbol{\varphi}\boldsymbol{\varphi}^T dz \right)$$

$$= \sum_i \sum_j \sum_k \int_A L_i \boldsymbol{L}\boldsymbol{L}^T dA \otimes \int_{t_{n-1}}^{t_n} N_{tj} \boldsymbol{\psi} \frac{\partial \boldsymbol{\psi}^T}{\partial t} dt \otimes \int_{z_{m-1}}^{z_m} N_{zk} \frac{\partial c_{ijk}}{\partial T_l} \boldsymbol{\varphi}\boldsymbol{\varphi}^T dz$$

$$= \sum_i \sum_j \sum_k \int_A L_i \boldsymbol{L}\boldsymbol{L}^T dA \otimes \int_{t_{n-1}}^{t_n} N_{tj} \boldsymbol{\psi} \frac{\partial \boldsymbol{\psi}^T}{\partial t} dt \otimes \int_{z_{m-1}}^{z_m} N_{zk} \frac{\partial c_{ijk}}{\partial T_{ijk}} \frac{\partial T_{ijk}}{\partial T_l} \boldsymbol{\varphi}\boldsymbol{\varphi}^T dz$$

where $\partial c_{ijk} / \partial T_{ijk}$ is the derivative of ρc with respect to the temperature at x_i, y_i, z_j, and t_k. This derivative is based upon the relation between the material properties and the temperature described in the material table. Since the temperature T_{ijk} is given as

$$T_{ijk} = \left[\boldsymbol{L}(x_i, y_i) \otimes \boldsymbol{\psi}(t_j) \otimes \boldsymbol{\varphi}(z_k)\right]^T \boldsymbol{T},$$

the derivative, $\partial T_{ijk} / \partial T_l$, is the coefficient of T_l in the above equation.

In the Newton-Raphson's iteration, Eq. (9) is first solved for the solution improvement $\Delta \boldsymbol{a}_{n,k}$ which is then updated based upon Eq. (10) to get a better solution. A Newton-Raphson's iteration will be restarted with the new solution until the error residual is reduced to an accepted level.

IV. NUMERICAL RESULTS

Several examples have been studied to verify the accuracy of the solution procedure, designed to solve the nonlinear finite element equations derived by the discontinous Galerkin's method for the heat transfer problems. To start the example problems, an exact solution of temperature is first selected, which gives zero temperature on the entire surface of the domain. That is, the example problems have zero boundary temperature. The heat source term, Q, that generates the prescribed temperature, can be obtained by substituting the given temperature function into the governing differential equation of Eq. (1). The material properties are assumed to be linear in temperature and in the form of $(a\,T + b)$.

The convergence criterion used in this study is defined that every component of the unknown vector, $\boldsymbol{a}^i$, should satisfy the condition

$$\frac{\left|a_j^i - a_j^{i-1}\right|}{\left|a_j^{i-1}\right|} < \alpha \tag{11}$$

IV. 1 One Dimensional Problem

The exact temperature field is given as

$$T(x,t) = t\sum_{n=2}^{5} n \cdot \phi_n(\eta)$$

The fifth order polynomial is used in the finite element equation to approximate the solution through thickness. The entire thickness is divided into three subdomains, in each of which the material properties will be expressed as a linear function of position and time.

Case 1: Effect of Nonlinearity

The constants in the assumed relation between the material properties and the temperature will be varied to study the effect of nonlinearity on solution accuracy. In this study, the material properties are assumed to be in the form of ($T + b$). The values of b ranges from 3 to 15. Since the maximal value of the temperature in this problem is around 2.5, the problem will experience less nonlinearity with a higher value of b.

Figure 2 shows the temperature solutions with various values of b. It is shown that, under the current discretization, the solution procedure is not able to reach at the correct solution when the nonlinearity is high. The results of numerical experiments also show that using the converged solution of the problem with less nonlinearity as the initial guess does not improve the solution accuracy of the problem with higher nonlinearity.

Case 2: Approximation of Time Axis

This case will study the effectiveness of the approximation along the time axis. The exact temperature field is given as a quadratic function of time as

$$T(x,t) = t^2\sum_{n=2}^{5} n\phi_n(\eta)$$

Figures 3 and 4 compare the calculated temperatures with the exact solution at time =1 and 2 seconds. The symbols **ipt**, **dt** and **nt** in the figures are referred to the order of polynomial of time, the time interval for each element and the number of subdomains along the time axis, respectively. It is shown that increasing **ipt** and **nt,** and reducing **dt** do not have significant impact on the accuracy of the solution.

IV. 2 Two Dimensional Examples

The domain of the problem is a $1 \times 1 \times 1$ slab. The exact solution is given as

$$T(x,t) = txy(x-1)(y-1)\sum_{n=2}^{5} n\phi_n(\eta)$$

The central plane of the slab is discretized into three models with 8, 32 and 128 triangular elements, respectively. These models are shown in Figs. 5 to 7. For most of the cases studied, a 5th order polynomial in z and a linear polynomial in time are used for interpolation. The material properties are in the form of $(T + 1)$. The convergence criterion of Eq. (11) is set to be 0.001. Finally, both of the time interval and the thickness are discretized into three subdomains.

Case 1: Better Approximation in Material Nonlinearity

Figures 8 and 9 shows the comparisons of results of the 8-element model reported at the center of the domain for three time instances. The results in Fig.8 are obtained with both the z and the time intervals being discretized into 3 subdomains, while those in Fig. 9 discretized into 6 subdomains. The results reveal that increasing the subdomains to better the approximation of the material properties does not uniformly improve the accuracy through the time and the spatial domains.

Similar studies are done with 32-element and 128-element models. The results are summarized in Figs. 10 and 11 and Figs. 12 and 13. Note that only the number of subdomains along the z interval is increased in these cases. Again, it is observed that increasing the number of points to better approximate the material nonlinearity may not necessarily result in an improvement in the solution accuracy everywhere.

Comparison of Figs. 8 and 9 to Figs. 10 and 11 and to Figs. 12 and 13 reveals another concern that reducing the size of the h elements does not improve the solution. Similar study, done on cases with linear material properties, draws a similar conclusion. The results are shown in Figs. 14 to 16. This observation leads to the next case of study.

Case 2: Reduction of h-size

The temperatures at the off-centered points, 59 and 61 on Fig. 7, are calculated and reported in Figs. 17 and 18, respectively. It is clear that the reduction of element size does not warrant an improved solution uniformly throughout the time and the spatial domains.

V. SUGGESTION FOR THE FUTURE STUDY

The initial study shows that more works need to be done in order to make the discontinous Galerkin's method an effective one for nonlinear transient problems. On one hand, one needs to develop a theoretical base to control the numerical errors in terms of orders of the polynomial and size of the elements. On the other hand, one needs to develop an effective method to approximate the material nonlinearly and to reduce computational cumbersome of the Jacobean matrices.

REFERENCE

1. Bey, K. S., personal communication, 1997

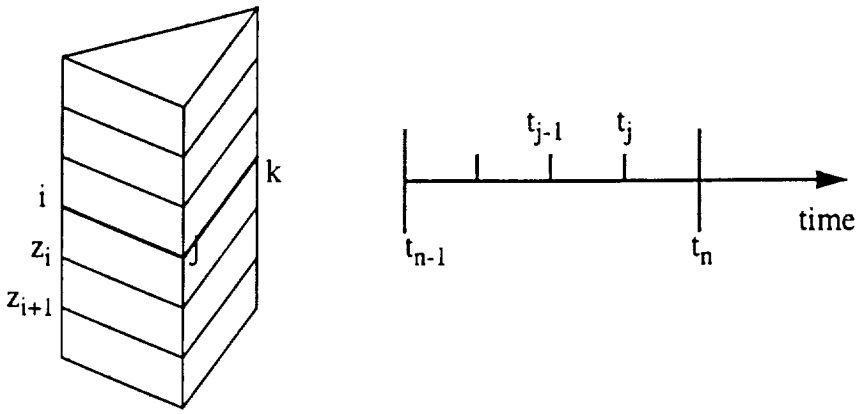

Figure 1. Subdomain in Spatial and Time Domains

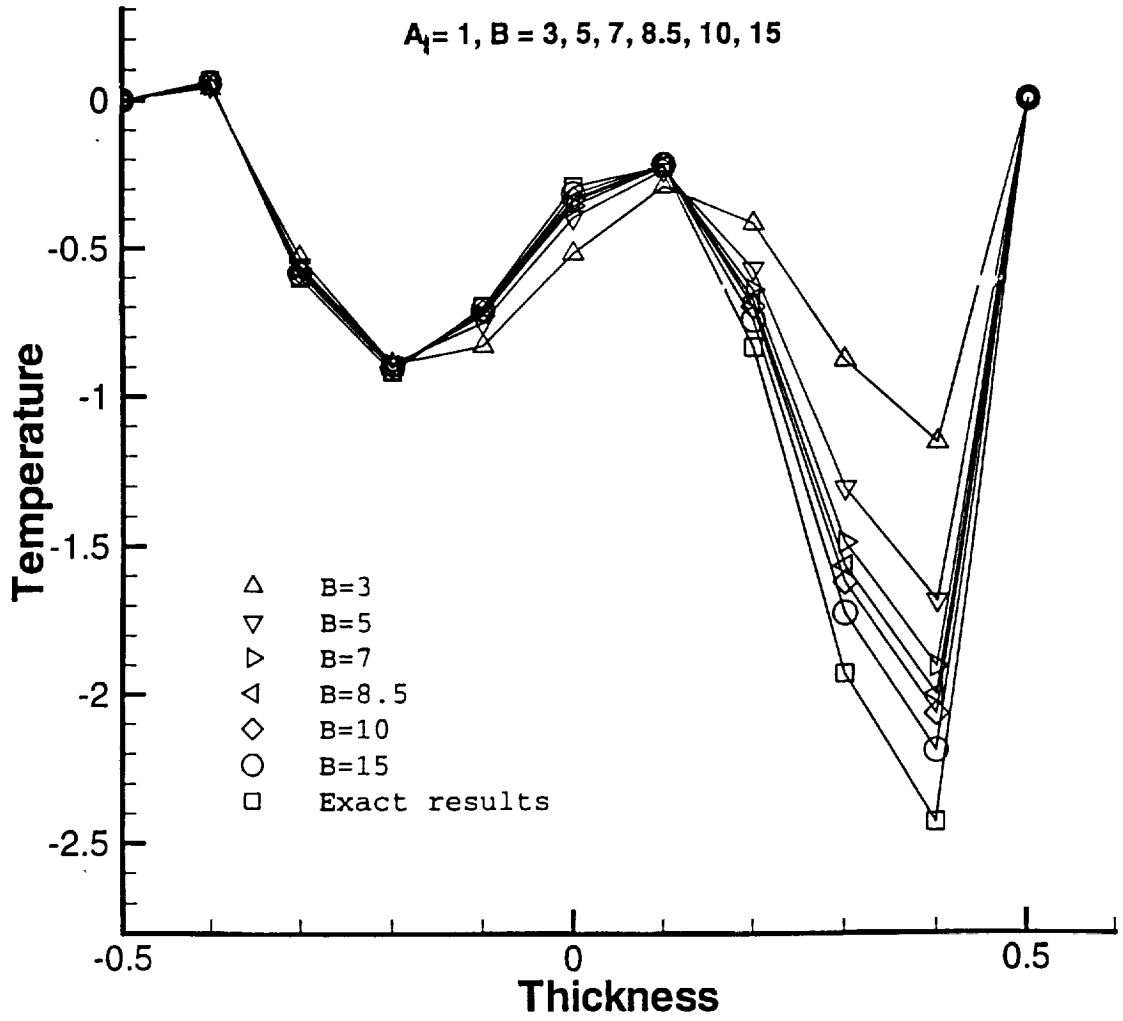

Figure 2. Accuracy of Solutions with Different Degrees of Nonlinearity

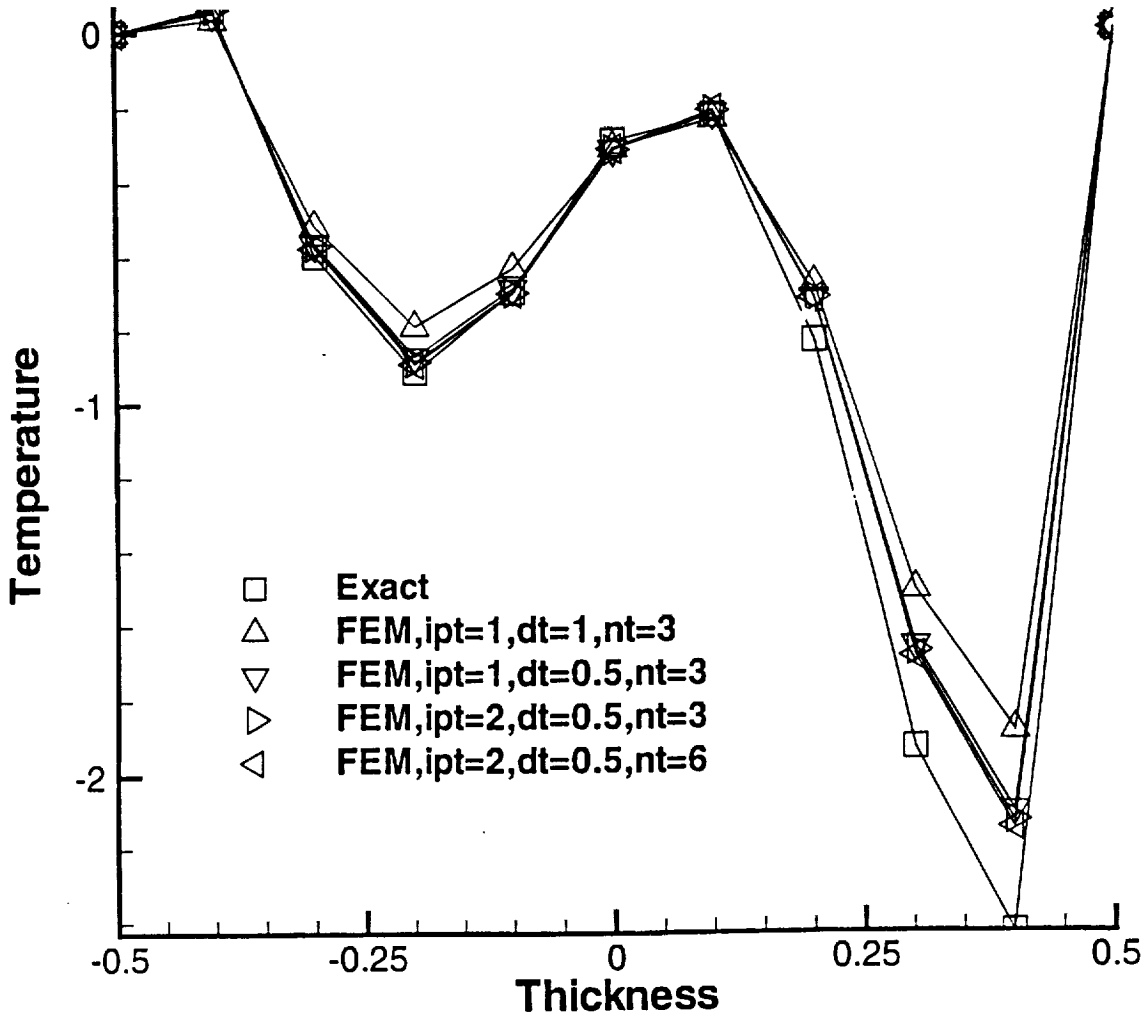

Figure 3. Different Approximation along Time Axis; Solutions at Second 1

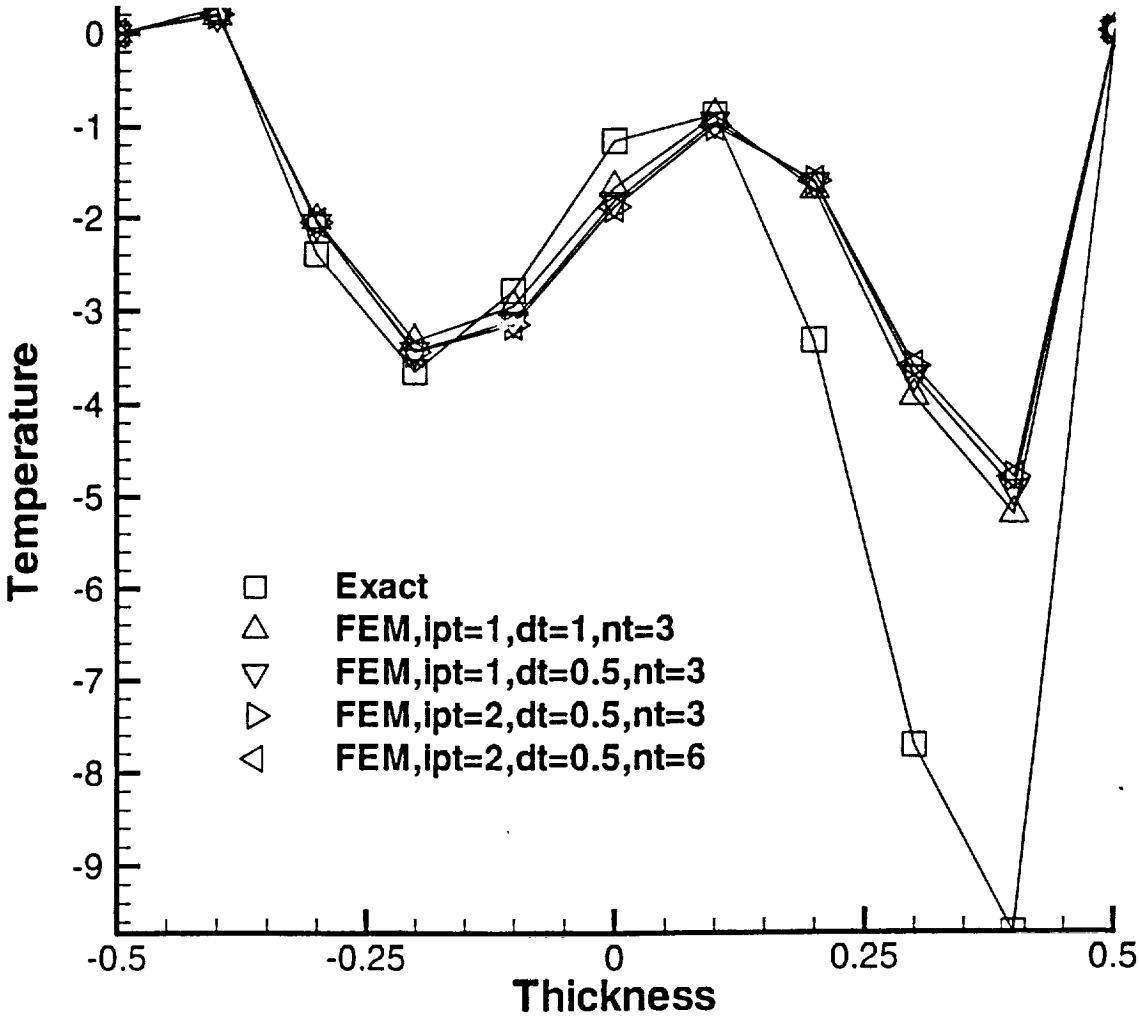

Figure 4. Different Approximation along Time Axis; Solutions at Second 2

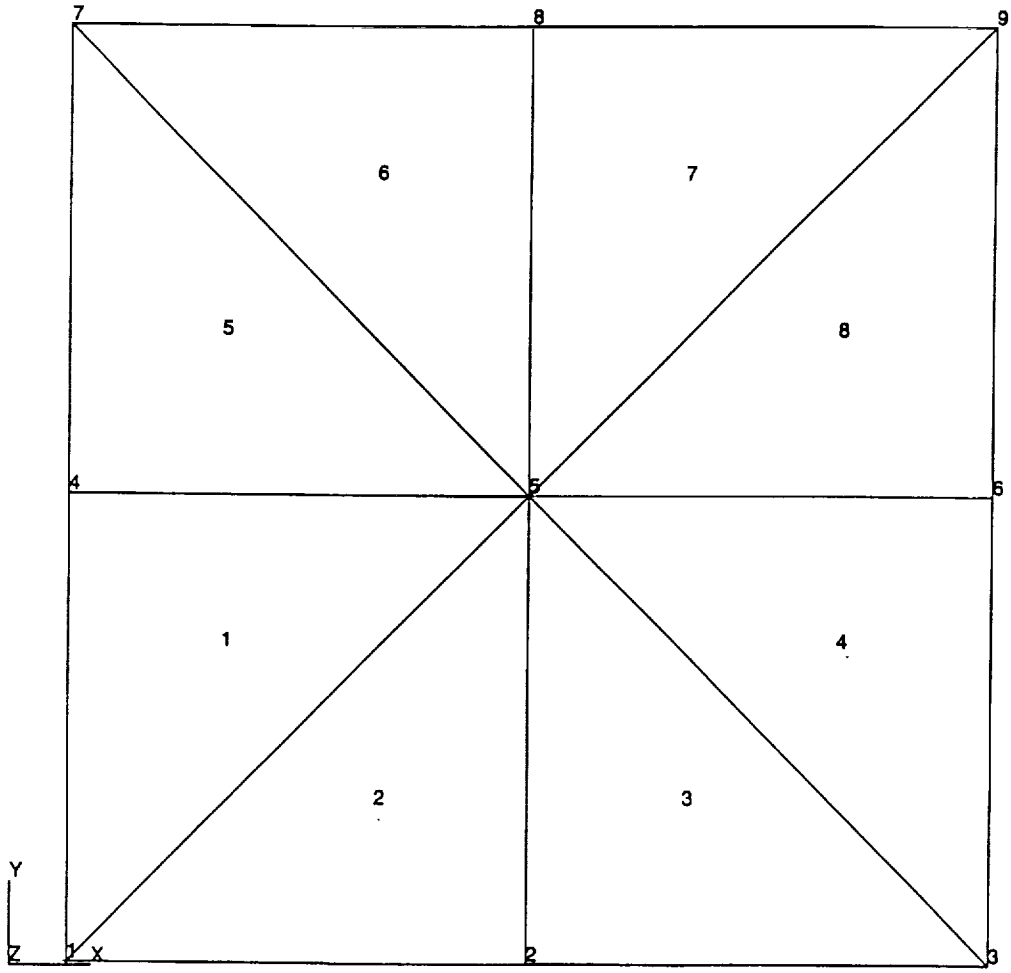

Figure 5. 8-Element Model

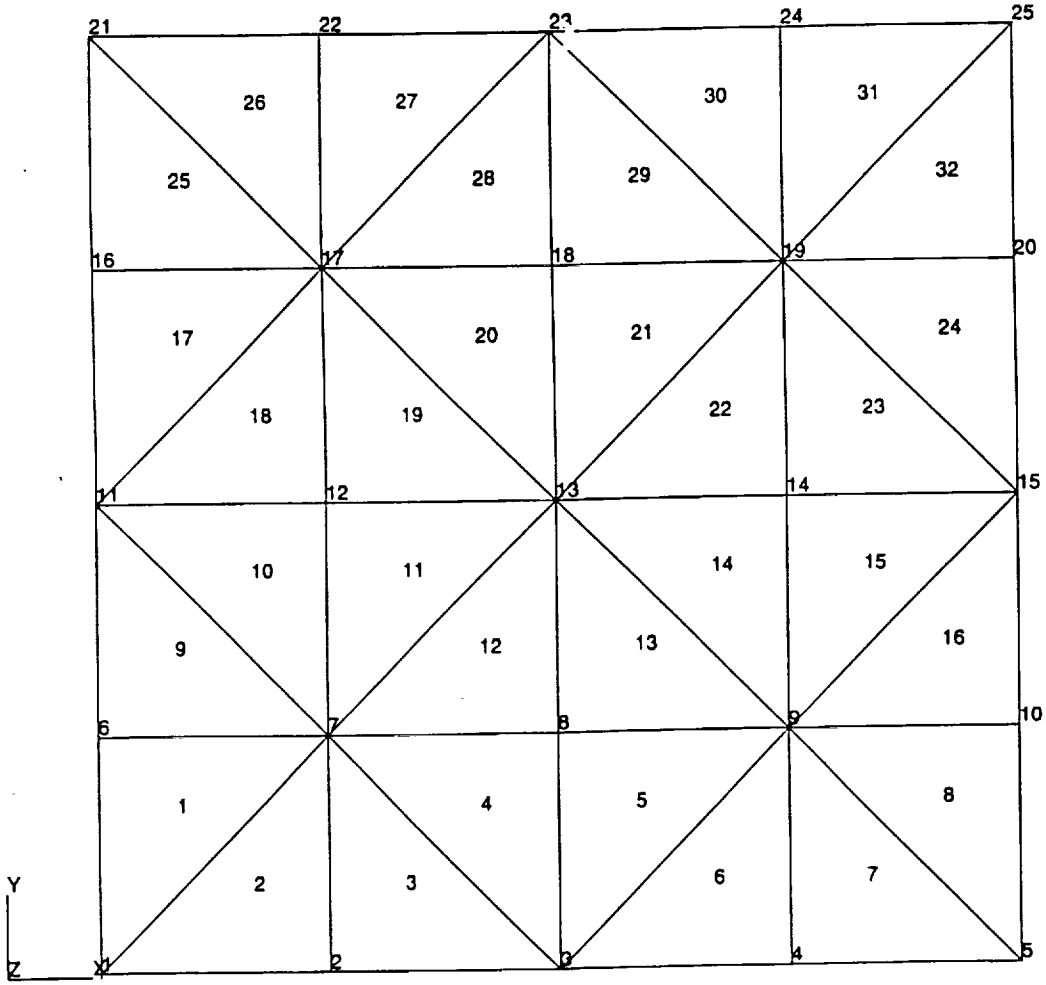

Figure 6. 32-Element Model

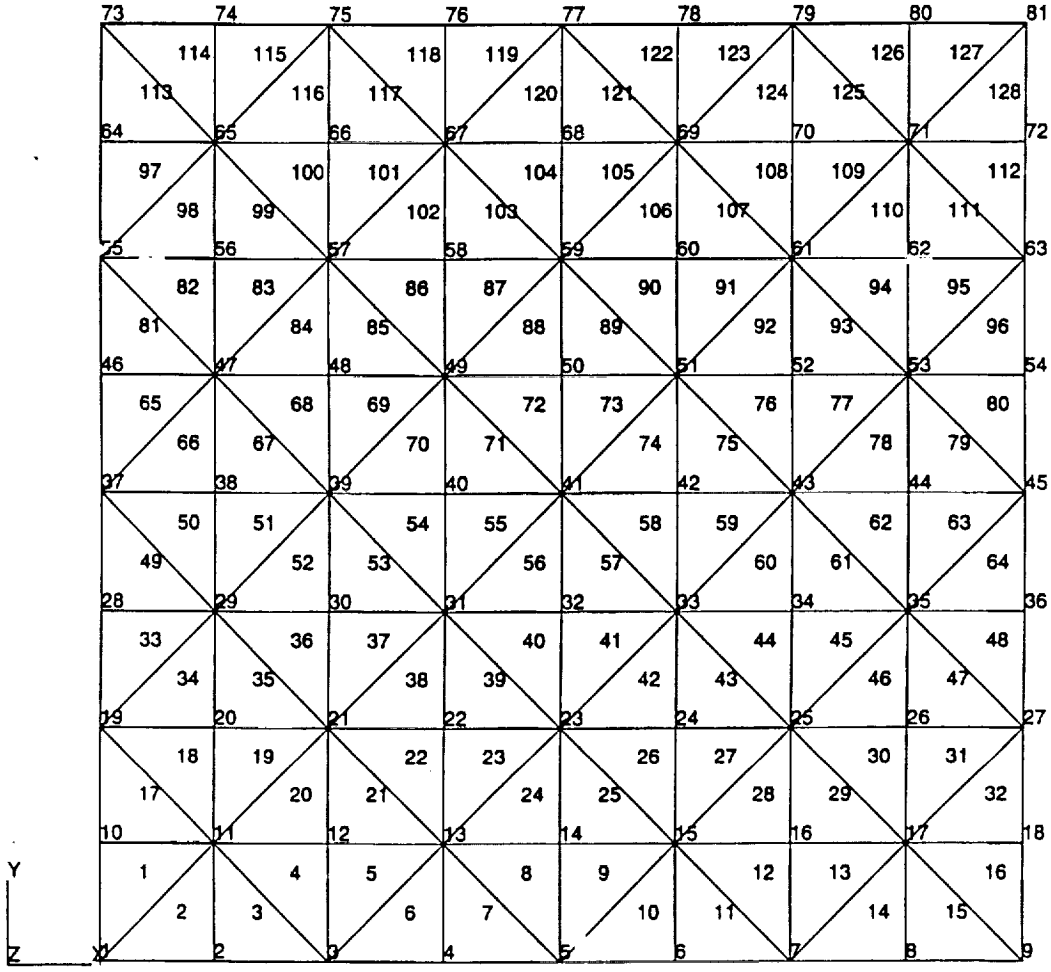

Figure 7. 128-Element Model

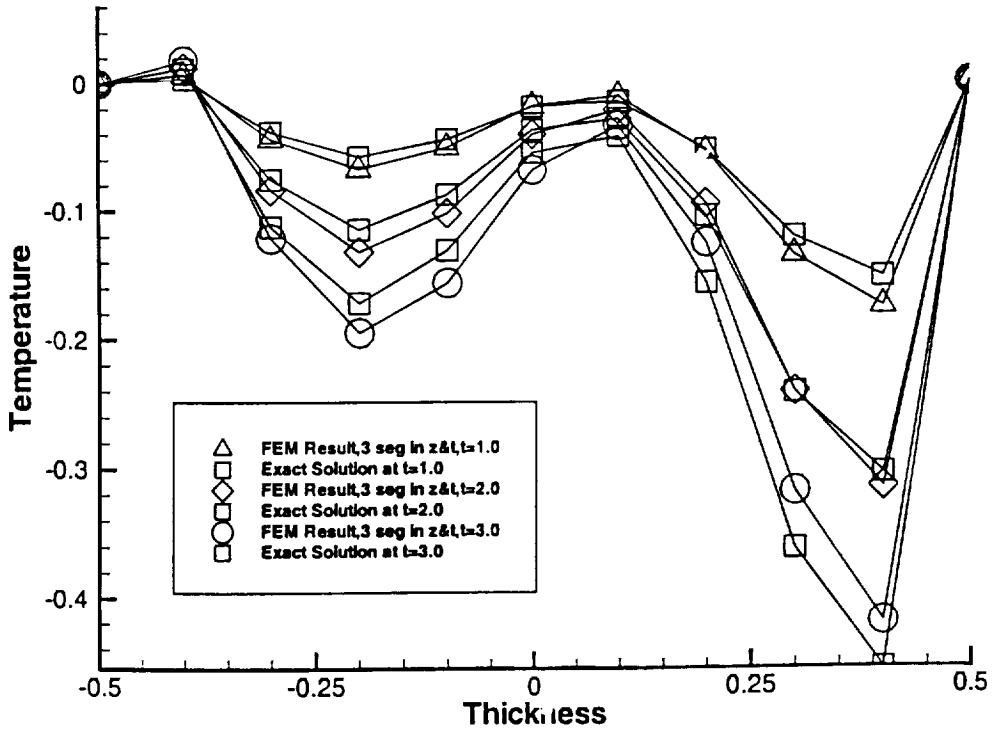

Figure 8. Solutions for 8-Element Model with 3 Subdomains in z and t

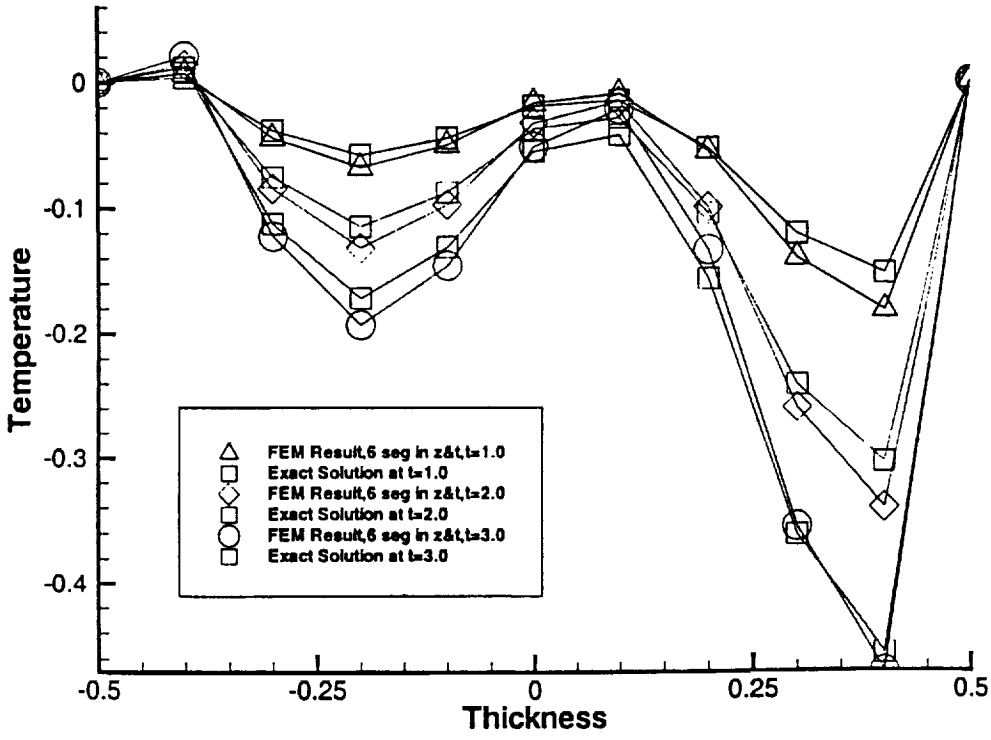

Figure 9. Solutions for 8-Element Model with 6 Subdomains in z and t

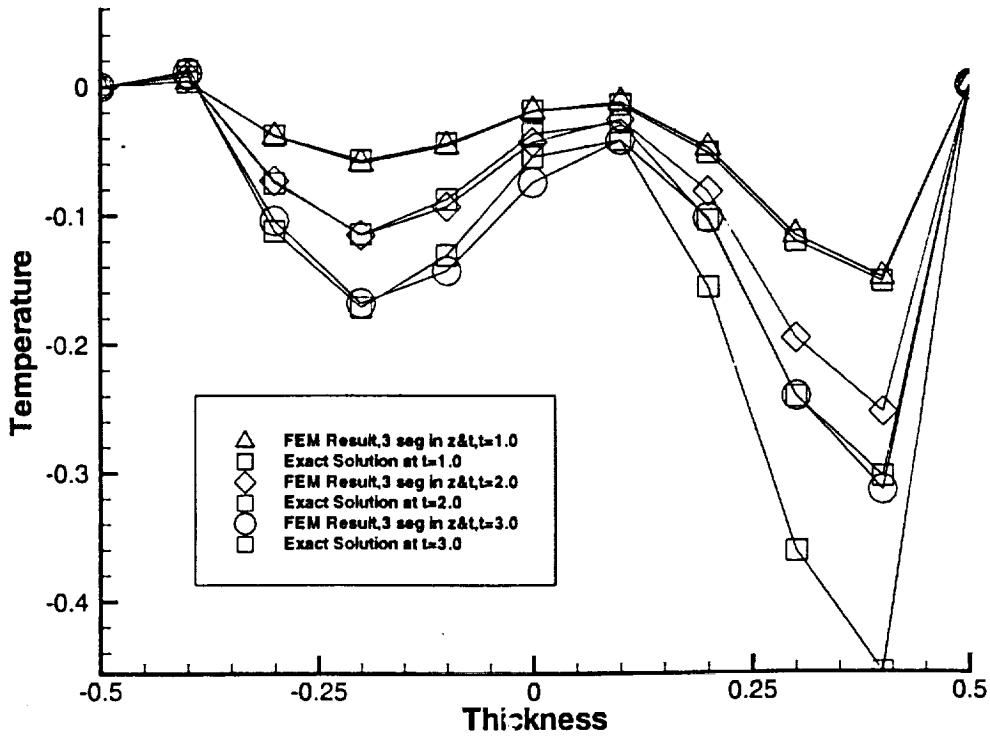

Figure 10. Solutions for 32-Element Model with 3 Subdomains in z and t

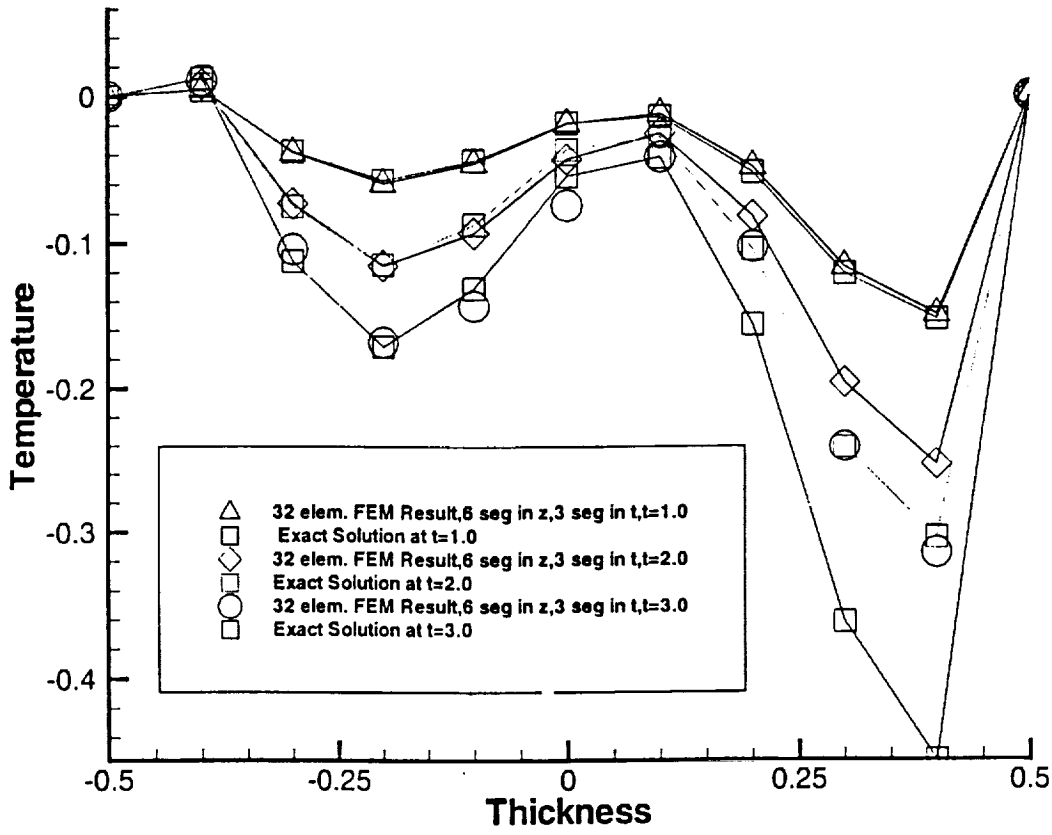

Figure 11. Solutions for 32-Element Model with 6 Subdomains in z and 3 Subdomains in t

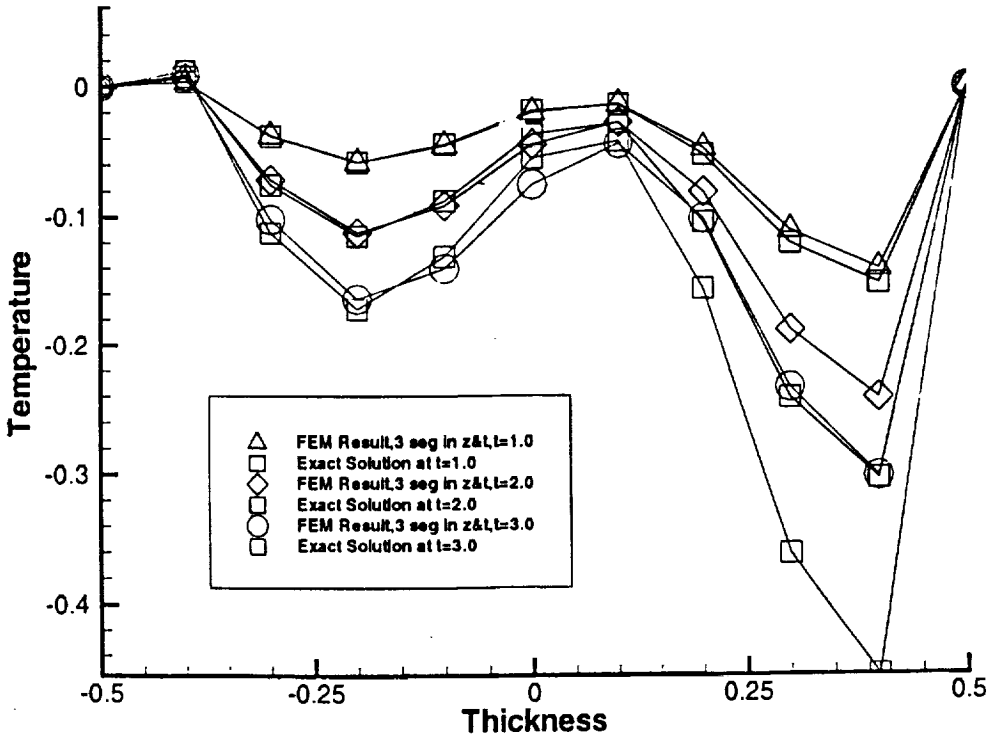

Figure 12. Solutions for 128-Element Model with 3 Subdomains in z and t

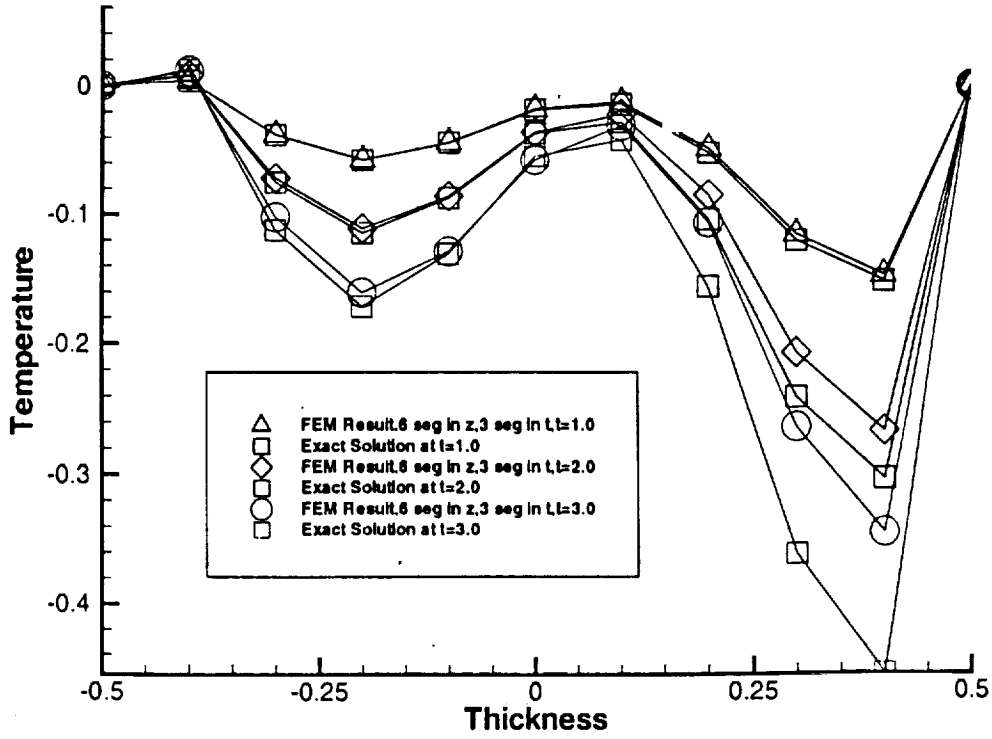

Figure 13. Solutions for 128-Element Model with 6 Subdomains in z and 3 Subdomains in t

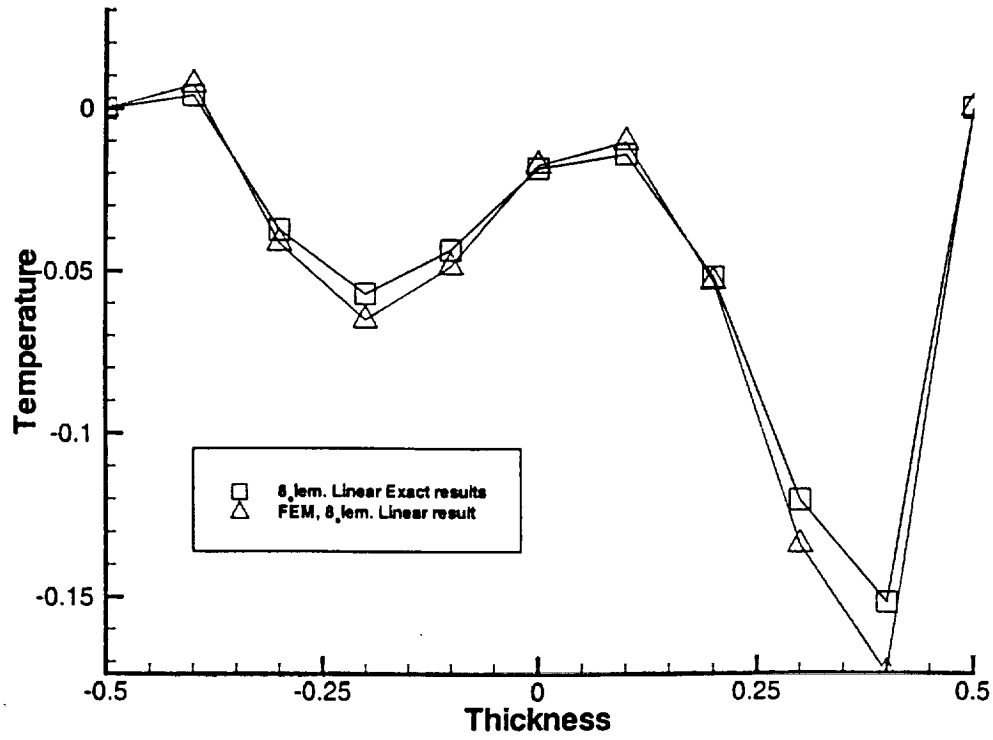

Figure 14. Linear Transient Solutions with 8-Element Model

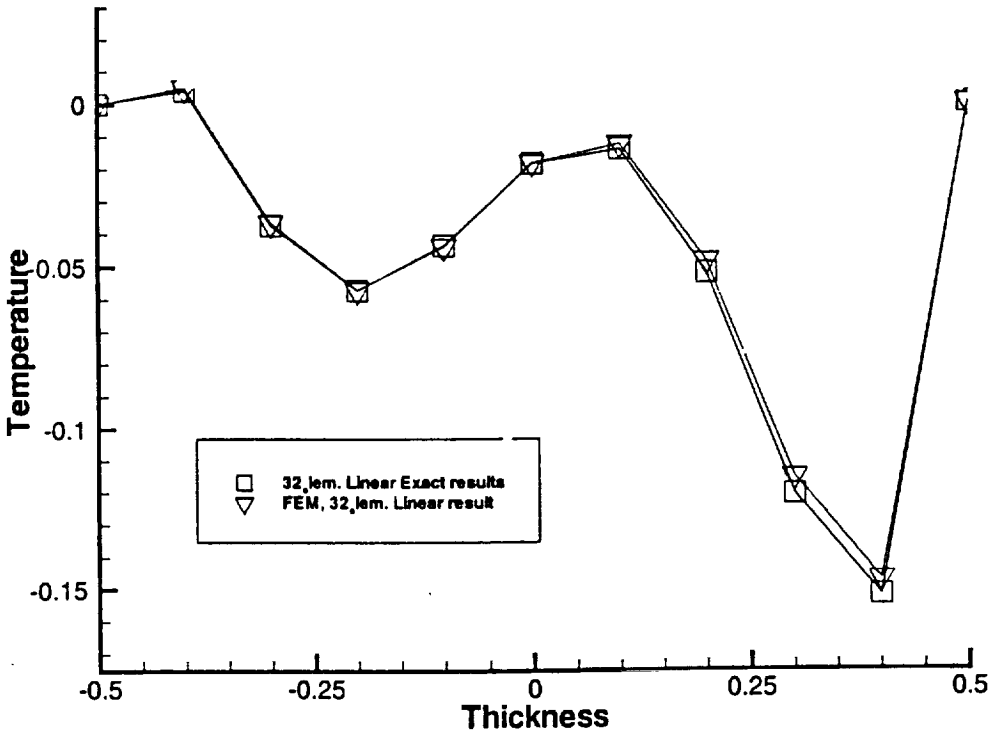

Figure 15. Linear Transient Solutions with 32-Element Model

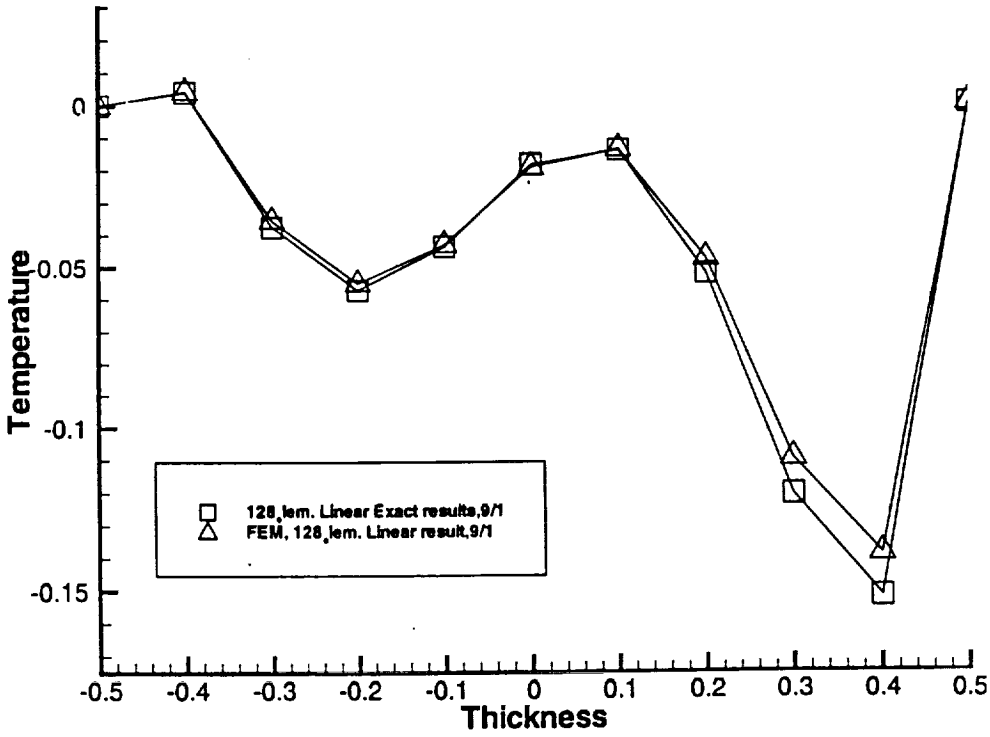

Figure 16. Linear Transient Solutions with 128-Element Model

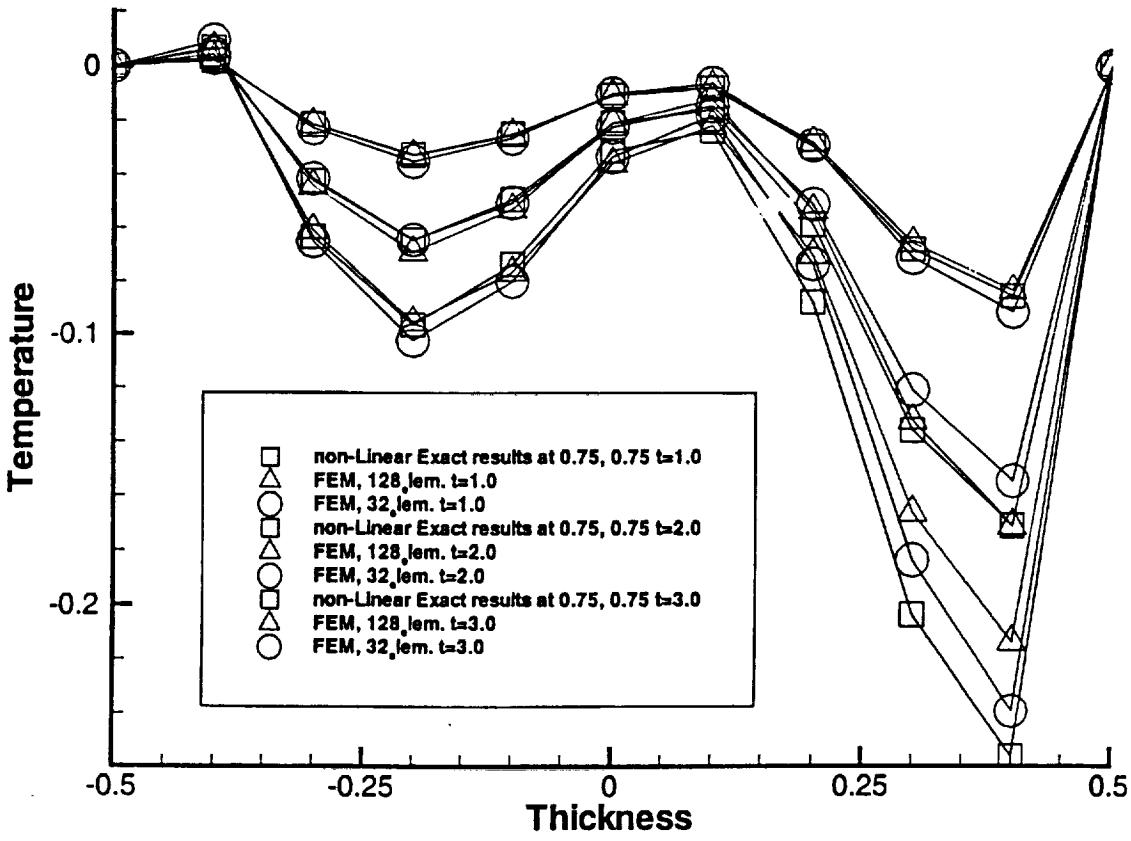

Figure 17. Comparison of Solutions at Point(x=0.75, y=0.75)

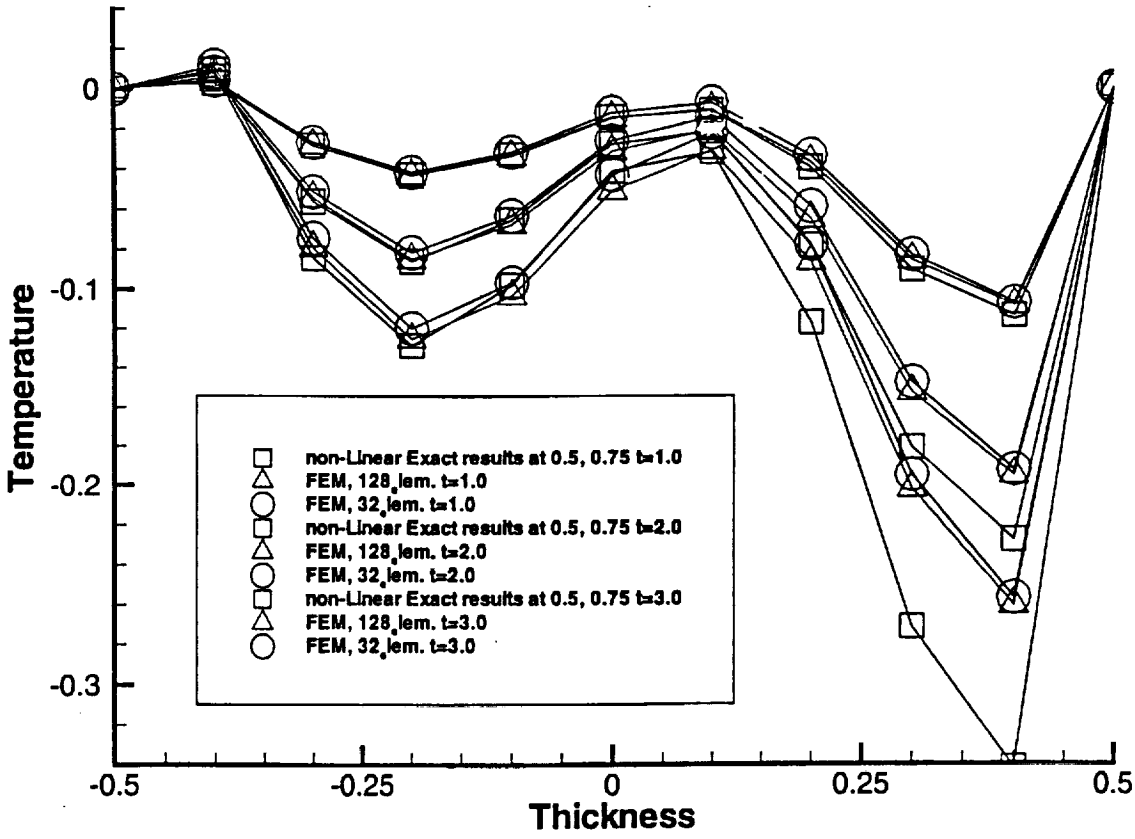

Figure 18. Comparison of Solutions at Point(x=0.5, y=0.75)